

Experimental Evidence of Multiple-Mirror Plasma Confinement*

B. Grant Logan, I. G. Brown, M. A. Lieberman, and A. J. Lichtenberg

Department of Electrical Engineering and Computer Sciences, and the Electronics Research Laboratory, University of California, Berkeley, California 94720

(Received 31 May 1972; revised manuscript received 18 September 1972)

Enhanced confinement of thermally ionized potassium plasma with increasing number of magnetic mirrors has been observed in a steady-state single-ended *Q* machine. The improved confinement occurs in an intermediate mean-free-path regime, and is in good agreement with theory.

In a previous Letter,¹ results of numerical computations on particle confinement in a multiple-mirror geometry were reported. In this Letter, experimental results are reported on multiple-mirror confinement in a steady-state, single-ended *Q* device, shown in Fig. 1. These experiments were conducted with a fixed multiple-mirror field of five mirror cells, each cell of length $l_c = 28$ cm, with a mirror ratio $M = B_{\max}/B_{\min} = 3.2$. Ions were created in the first mirror throat by contact ionization of lithium or potassium vapor on a hot tungsten plate, which also provided electrons for the plasma by thermionic emission. The plasma length L and the number of mirror cells $K = L/l_c$ was varied by axially moving a negatively biased collector plate within the fixed field. All experiments were conducted in stable regimes in which the fluctuation levels were low ($\delta n/n \leq 1\%$). However, some radial loss persisted, probably because of convection from hot-plate temperature inhomogeneities. The chamber was evacuated to less than 5×10^{-6} Torr, so that ion-neutral collisions were negligible compared to ion-ion collisions at the lowest plasma densities in the experiment. Volume recombination was negligible.

At low densities for which the ion-ion scatter-

ing mean free path (mfp) is comparable to or longer than the system length L , most ions pass through the system adiabatically. If there are no radial losses, the densities at corresponding points in all cells are nearly the same, and the ion confinement time τ increases proportionately with the transit time L/\bar{v}_i , where \bar{v}_i is the ion thermal velocity.

At intermediate densities for which the mfp is much less than L and comparable to l_c , repetitive trapping and detrapping of ions by the multiple mirrors is expected to result in axial diffusion of ions, and an axial density gradient results with the density increasing toward the source.¹⁻³ For Maxwellianization in all cells and large mirror ratios, the density in the midplane of the first cell (next to the source) has an upper limit, in the absence of recombination and radial loss, given by

$$n_1 = K\Delta n = (L/l_c)\Delta n \quad (K \geq 1), \tag{1}$$

where Δn is the density increment across each mirror.³ With a resulting average density $\bar{n} \approx \frac{1}{2}n_1$ for the entire system, the confinement time using Eq. (1) is

$$\tau_x \approx \frac{1}{2}n_1 L/S \approx \frac{1}{2}\Delta n L^2/l_c S, \tag{2}$$

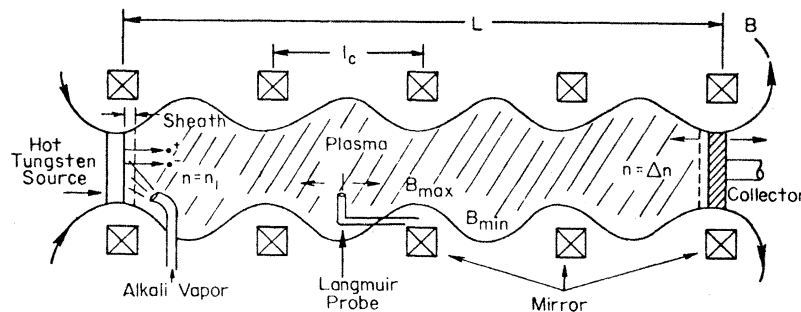


FIG. 1. The multiple-mirror confinement experiment.

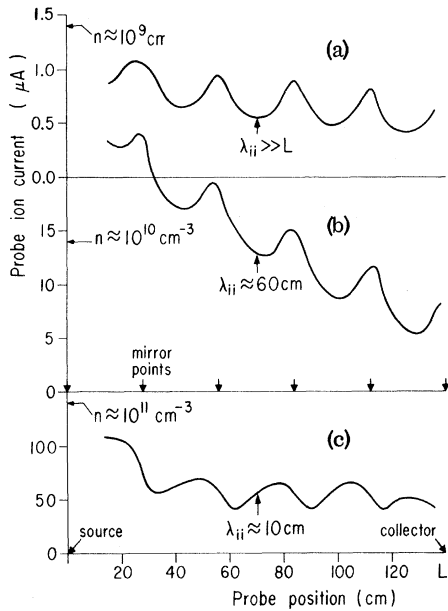


FIG. 2. Langmuir-probe ion saturation current as a function of axial position, for (a) long-, (b) intermediate-, and (c) short-mfp regimes.

where S (ions/cm² sec) is the source flux density. We note from Eq. (2) that $\tau \propto L^2$ in the intermediate-mfp regime.

At high densities for which $mfp \ll B(dB/dz)^{-1}$, the mirror width, a theory of magnetohydrodynamic (MHD) flow in an ideal multiple-mirror system predicts uniform flow conditions at corresponding points in all cells.⁴ Thus, the confinement time scales according to the transit time L/\bar{v}_d , where \bar{v}_d is the mean macroscopic plasma flow velocity.

In Fig. 2, typical axial profiles of Langmuir-probe ion saturation current are presented for (a) the long-mfp regime, (b) the intermediate-mfp regime, and (c) the MHD regime. From estimates of the ion temperature (kT_i > hot-plate temperature from nonequilibrium theory⁵), the density and mfp are indicated for the middle cell in each case. Corresponding to these three density regimes are measurements of total axial particle flux on a collector as a function of axial position, as given in Fig. 3. From the collector signals in Fig. 3 we observe that, except for the anomalous loss in the first cell, there is a gradual decay of the axial particle flux indicating a moderate rate of radial loss. For the long-mfp regime, comparing Figs. 2(a) and 3(a), we find that the midplane density falls only slightly fast-

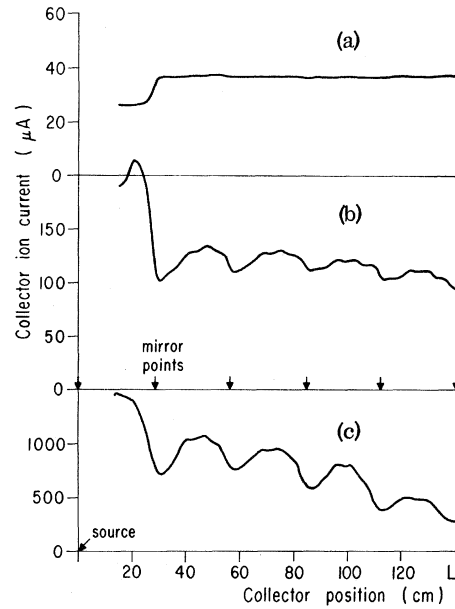


FIG. 3. Collector ion saturation current as a function of distance from the source for (a) long-, (b) intermediate-, and (c) short-mfp regimes.

er than the collector signal, thus indicating that there is little multiple-mirror action. The axial density is a minimum in the mirror centers and a maximum in the mirror throats as expected when collision rates are low. In contrast, for the intermediate-mfp regime, given in Figs. 2(b) and 3(b), the midplane density falls stepwise from cell to cell, in rough agreement with Eq. (1), indicating strong multiple-mirror action. Finally, in Fig. 2(c), the density is nearly constant from cell to cell, characteristic of MHD flow. The density is now a minimum at mirror throats, rather than in the mirror midplanes, another characteristic of MHD flow.⁴

By definition, the containment time is the total number of ions within the system, divided by the input flux:

$$\tau \equiv \frac{\int_0^L n(z) dz}{I_c(0)/eA}, \quad (3)$$

where $I_c(0)$ is the collector current at the hot plate, and A is the effective plasma area in that plane. By measuring $n(z)$ and $I_c(0)$, we can determine the containment time τ . From Figs. 2 and 3, and from similar data at other densities, the result is given as the dashed curve in Fig. 4. The values of τ , calculated in this way, include all sources of loss. Adding the major sources of

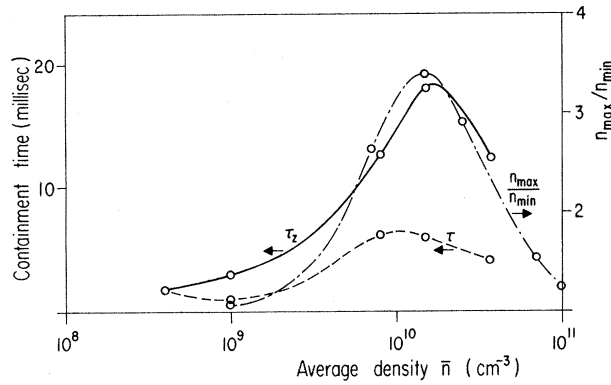


FIG. 4. Total confinement time τ (dashed line), longitudinal confinement time τ_z (solid line), and first-cell density-ratio n_{\max}/n_{\min} (dash-dotted line) as functions of average density \bar{n} .

loss we have

$$\tau^{-1} = \tau_z^{-1} + \tau_{\text{rad}}^{-1} + \tau_{\text{rec}}^{-1}, \quad (4)$$

where τ_{rad} is the radial loss, τ_{rec} is the recombination loss on the hotplate, and τ_z is the axial loss to the collector. For potassium operating well in the electron-rich regime, τ_{rec} is greater than 10τ , and is neglected. Taking the collector current at the end of the multiple mirror to be given by

$$\frac{I_c(L)}{eA} = \frac{I_c(0)}{eA} - \frac{1}{\tau_{\text{rad}}} \int_0^L n(z) dz, \quad (5)$$

and substituting for the integral from (3), solving for τ and substituting the result in (4), we obtain

$$\tau_z = \tau I_c(0)/I_c(L). \quad (6)$$

We can use this result together with the collector data to obtain the results for τ_z as given by the solid line in Fig. 4. These experimental results can be compared with the theoretically maximum containment times in the three regimes. Taking the ion velocity $v_i \approx 2 \times 10^5$ cm/sec and the average mirror ratio $\bar{M} = 2.5$, which are the experimental parameters, we find in the free-flow regime $\tau_{\text{ff}} = L/v_i = 0.7$ msec,² in the multiple-mirror regime $\tau_{\text{mm}} = 2\bar{M}KL/v_i = 17.5$ msec,² and in the MHD regime $\tau_{\text{MHD}} = 2\bar{M}L/v_i = 3.5$ msec,⁴ which agree well with our experimental results. In the low- and high-density regimes there is considerable multiple-mirror trapping such that the confinement times there are above the free-streaming and MHD limits. We can also compare the confinement time in the multiple-mirror regime with the upper limit for a single mirror

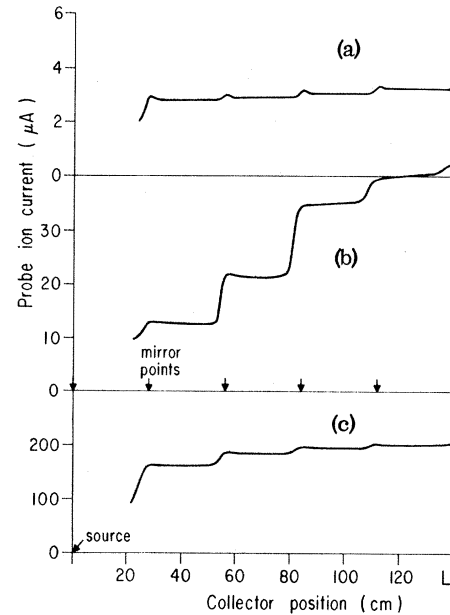


FIG. 5. Langmuir-probe ion saturation current in the first-cell midplane as a function of collector position, in the (a) long-, (b) intermediate-, and (c) short-mfp regimes.

$\tau_{\text{sm}} = 4\bar{M}L/v_i = 7$ msec,² conclusively demonstrating, experimentally, the existence of the multiple-mirror effect.

A test of the scaling law of multiple-mirror confinement can also be made by observing the change in density within a fixed cell as the number of mirrors is increased. For a constant source strength, an improvement in confinement results in an increase in density. In Fig. 5 the density n_1 measured by a Langmuir probe fixed in the midplane of the first cell adjacent to the source is shown as a function of the distance of the collector from the source. Thus, as the collector is withdrawn, mirror cells are added to the system. Figures 5(a)–5(c) are, respectively, for a long-, intermediate-, and moderately short-mfp regimes. The density n_1 jumps at each point where the collector passes a mirror throat. In Figs. 5(a)–5(c), the first density jump corresponding to the collector passing the second throat (the source being located in the first throat) is a result of partial filling of velocity space at the midplane due to mirror trapping in the first cell. It is not a multiple-mirror effect, and only jumps following the first are used as a measure of improvement in confinement with multiple mirrors over the confinement with one mirror cell.

The enhancement in density is greatest in the intermediate-mfp regime [Fig. 5(b)] as predicted by the theory. In Fig. 5(b) the magnitude of the density jump decreases with each additional mirror. According to Eq. (2), the measured increases in n_1 as the number of cells is increased corresponds to a confinement time τ scaling as L^2 for the first three cells, relaxing to L as more cells are added. This is to be expected in the presence of recombination loss and radial loss, which becomes more important as the confinement time due to multiple-mirror action increases. The ratio of n_1 with five mirror cells (n_{\max}) to n_1 with one mirror cell (n_{\min}) is plotted as a dash-dotted curve in Fig. 4. It is seen to follow generally the values of τ_z .

*Research sponsored by the National Science Foundation under Grant No. GK-27538, and by the U. S. Air Force Office of Scientific Research under Grant No. AF-AFOSR-69-1754. One of the authors (B.G.L.) held a U. S. Atomic Energy Commission Fellowship.

¹B. Grant Logan, A. J. Lichtenberg, M. A. Lieberman, and A. Makhijani, *Phys. Rev. Lett.* **28**, 144 (1972).

²B. Grant Logan, Fourth Quarterly Progress Report on Plasma Research, Electronics Research Laboratory, University of California, Berkeley, 1969 (unpublished).

³G. I. Budker, V. A. Mirnov, and D. D. Ryutov, *Pis'ma Zh. Eksp. Teor. Fiz.* **14**, 320 (1971) [*JETP Lett.* **14**, 212 (1971)].

⁴A. Makhijani, Second Semiannual Progress Report on Plasma Research, Electronics Research Laboratory, University of California, Berkeley, 1971 (unpublished).

Parametric Instability and Anomalous Heating Due to Electromagnetic Waves in Plasma*

M. Porkolab, V. Arunasalam, and R. A. Ellis, Jr.

Plasma Physics Laboratory, Princeton University, Princeton, New Jersey 08540

(Received 28 September 1972)

Experimental results are presented which verify the fundamental aspects of the parametric instability of whistler waves. The accompanying fast heating of plasma is interpreted to be due to anomalous absorption.

In this Letter we present experimental results which show (i) the parametric decay of a large-amplitude electron cyclotron wave (whistler) and/or an electron plasma wave in a plasma in a magnetic field; and (ii) the associated anomalous heating of both electrons and ions. In addition, the decay spectrum and the heating were measured as the incident microwave power, the pulse duration, and the magnetic field strength were varied. Although recently predicted by theory,¹⁻³ to our knowledge, this is the first time that the parametric decay and associated plasma heating due to whistler waves have been measured in laboratory experiments.

The experiments were carried out in the 3-m-long Princeton L-3 linear device. The plasma was produced in the steady state by a 5-cm-diam, 20-cm-long helical slow wave structure,⁴ which injected up to 1 kW S-band microwave power into a magnetic mirror configuration. In the present experiments $f_0 = 2.45$ GHz, $f_{ce} = 2.45$ to 5.0 GHz, $f_{pe} \geq 10$ GHz, so that $f_0 \leq f_{ce} < f_{pe}$ (where f_{ce} and f_{pe} are the electron cyclotron and the electron

plasma frequencies, respectively). Recently Lisitano, Fontanesi, and Bernabei proposed that such structures heat the plasma nonresonantly by excitation and collisional absorption of electron waves.⁵ However, in our device we find that such nonresonant plasma sources operate in two modes; (1) at low pressures (i.e., $p \leq 10^{-3}$ Torr in He gas) and low densities ($n_0 \leq 2 \times 10^{12}$ cm⁻³), long-wavelength ($\lambda_{\parallel} \approx 3$ to 10 cm, $\lambda_{\perp} \approx 5$ cm) electron plasma waves are excited which obey the dispersion relation

$$1 = \omega_{pe}^2 \cos^2 \theta / \omega^2 + \omega_{pe}^2 \sin^2 \theta / (\omega^2 - \omega_{ce}^2), \quad (1)$$

where $\cos \theta = k_{\parallel} / k$, $\sin \theta = k_{\perp} / k$, and $k_{\parallel} = \vec{k} \cdot \vec{B} / B$. These waves decay parametrically into short-wavelength electron plasma waves [also satisfying Eq. (1)] and ion acoustic waves which propagate at an angle to the external magnetic field. These results are in agreement with recent theoretical predictions.^{1,2} (2) At higher pressures ($p \geq 2 \times 10^{-3}$ Torr in He gas) and higher densities ($n_0 \geq 3 \times 10^{12}$ to 10^{13} cm⁻³) whistler waves with wavelengths $\lambda_{\parallel} = 0.7$ to 2.5 cm, $\lambda_{\perp} \approx 5$ cm are